*Manuscript
Click here to view linked References

Main characteristics of Al_2O_3 thin films deposited by magnetron sputtering of an Al_2O_3 target at different RF power and argon pressure and their passivation effect on *p*-Si wafers

J.A. García-Valenzuela[a]*, R. Rivera[a,†], A.B. Morales-Vilches[b,‡], L.G. Gerling-Sarabia[b], A. Caballero[a], J.M. Asensi[a], C. Voz[b], J. Bertomeu[a], J. Andreu[a]

[a] *Departament de Física Aplicada, Universitat de Barcelona (UB), Carrer de Martí i Franquès 1-11, C.P. 08028, Barcelona, Catalonia, Spain.*

[b] *Departament d'Enginyeria Electrònica (DEE), Universitat Politècnica de Catalunya (UPC), Carrer de Jordi Girona 1-3, C.P. 08034, Barcelona, Catalonia, Spain.*

* Corresponding author. Tel.: +34 934 039221; fax: +34 934 039218.
E-mail addresses: jgarciavlz@ub.edu, jgarciavlz@gmail.com (J.A. García-Valenzuela).

† present address: *Sección de Fisicoquímica, Departamento de Química, Universidad Técnica Particular de Loja (UTPL), Calle París S/N, A.P. 11-01-608, Loja, Loja, Ecuador.*

‡ present address: *Kompetenzzentrum Dünnschicht- und Nanotechnologie für Photovoltaik Berlin (PVcomB), Helmholtz-Zentrum Berlin für Materialen und Energie (HZB) GmbH, Schwarzschildstraße 3, D-12489, Berlin-Adlershof, Germany.*

Abstract

In this work, 50-nm Al_2O_3 thin films were deposited at room temperature by magnetron sputtering from an Al_2O_3 target at different RF power and argon pressure values. The sputtering technique could be preferred to conventional atomic layer deposition for an industrial application, owing to its simplicity and higher deposition rate. The resulting thin films were characterized by UV/Vis/NIR spectroscopy, X-ray diffraction, and X-ray photoelectron spectroscopy. The deposited Al_2O_3 material was always highly transparent and amorphous in nature. It was found that the O/Al ratio is higher when the Al_2O_3 layer is deposited at lower RF power or higher argon pressure. Also, some argon incorporation into the films was observed at low deposition pressure. On the other hand, the performance of the previously characterized Al_2O_3 thin films in the passivation of 2.25 Ωcm *p*-type float zone *c*-Si wafer surfaces was evaluated by the quasi-steady-state photoconductance technique. The best effective carrier lifetime value at one-sun illumination, 0.34 ms (corresponding to a surface recombination velocity of 41 cm/s), was obtained with the 50-nm Al_2O_3 deposited at the higher argon pressure studied, 0.67 Pa (5.0 mTorr), with the lowest RF power studied, 150 W, and after an annealing process, in this case at 350 ºC for 20 min with forming gas. It was assumed that the reduction of the surface passivation quality at higher RF power or lower argon pressure is a consequence of an increased surface damage, and, probably, to a decrease of the O/Al ratio. These assumptions were confirmed with the obtainment of a lifetime of 0.73 ms (a surface recombination velocity equal to 19 cm/s) with a simple experiment with Al_2O_3 deposited with continuously varied sputtering conditions starting from minimal silicon surface damage conditions: 50 W and 6.67 Pa (50 mTorr). Finally, comments about further improvement of the effective lifetime (up to 1.25 ms, corresponding to a surface recombination velocity of 11.2 cm/s) with preliminary experiments about the incorporation of an intrinsic hydrogenated amorphous silicon interlayer are included.

Keywords: Alumina; Sputtering; RF power; Silicon; Surface passivation; Quasi-steady-state photoconductance; Lifetime.

1. Introduction

Nowadays, crystalline silicon (*c*-Si) and polycrystalline silicon (poly-Si) wafers constitute most of the solar cell technology, having the highest market share. The efficiency of *c*-Si solar cells is, however, reduced by recombination of photogenerated carriers at the silicon wafer surfaces. This aspect is gaining relevance, as thinner wafers (<200 μm) are progressively introduced in production lines. Therefore, the reduction of this surface recombination, called surface passivation, is very important in the performance of low-cost and high-efficiency *c*-Si solar cells.

It is known that the surface passivation can be achieved by means of two different strategies [1–7]. The first of them, called chemical passivation, refers to the reduction of interface state density (D_{it}) at the silicon surface, which can be achieved, for example, through the passivation of silicon dangling bonds by hydrogen atoms. The second one, called field-effect passivation, which consists of producing a band bending at the silicon surface, refers to the reduction in the density of one type of minority charge carrier present at the silicon surface by an electric field; this can be obtained, for example, by fixed charge (Q_f) present in the thin film deposited on the silicon surface. Among the common passivation thin films, the Al_2O_3 is currently gaining relevance [1–11] (thanks to the works of Agostinelli *et al.* [12] and Hoex *et al.* [13], both reported in 2006), since the passivation by this material, particularly by that deposited by atomic layer deposition (ALD) technique, is typically a combination of both chemical and field-effect passivation mechanisms [2,3]. This material contains a very high density of negative charges—high Q_f—and, as an inherent effect of the ALD technique, acts as a hydrogen reservoir providing hydrogen atoms to the $Si/SiO_x/Al_2O_3$ interface formed or restructured during thermal treatments, thus reducing D_{it}.

Although ALD-deposited Al_2O_3 shows the better passivation results, the ALD technique is not currently appropriate for large-scale production because of a limited throughput. The deposition rate of Al_2O_3 by conventional ALD equipments is typically below than 0.5 nm/min. However, the high-rate spatial ALD can overcome this limitation, but at the expense of higher system cost and complexity [14]. Nevertheless, the present film deposition industry is dominated by other techniques, such as magnetron sputtering. However, this industrially suitable technique, in comparison to the ALD one, has not been extensively studied in relation to the *c*-Si passivation by Al_2O_3, maybe due to the relatively lower surface passivation quality usually obtained [8–10]. In this regard, Cuevas and collaborators took the challenge of improving the passivation of *c*-Si by means of Al_2O_3 deposited by sputtering, and demonstrated in a sequence of papers [15–20] that such a material deposited by radio-frequency (RF) sputtering is suitable of providing good silicon surface passivation. However, a complete correlation between deposition conditions and the resulted passivation is lacking to date. Furthermore, the experiments by the group of Cuevas were developed exclusively with reactive sputtering of an Al target.

Therefore, in this paper we present a study of the main characteristics of Al_2O_3 thin films deposited by RF sputtering of an Al_2O_3 target under different RF power and deposition pressure values, and the passivation of *c*-Si wafers obtained by the effect of these Al_2O_3 deposited under the studied sputtering conditions. Specifically, we are focused on the overall effect of the mentioned sputtering parameters on the passivation of *p*-type *c*-Si by the deposited Al_2O_3, and, where possible, in the correlation of the Al_2O_3 characteristics with the passivation results of *p*-type *c*-Si wafers, according to the studied sputtering conditions. It is expected that the results lead to a better understanding of the passivation of *c*-Si wafers due to the sputtering-deposited Al_2O_3, and thus allows designing a scheme to improve the passivation results by this current industry dominant deposition technique.

2. Experimental details

The experimental design for developing this work is divided into two subsections: 1) the synthesis and routine characterization of the Al_2O_3 thin films deposited on glass substrates, and 2) the passivation effect of such Al_2O_3 thin films deposited on the *p*-Si wafer surfaces, assessed from the measurements of the carrier lifetimes.

2.1. Synthesis and characterization of Al_2O_3 deposited on glass substrates

The Al_2O_3 thin films were deposited at room temperature onto 5×5 cm^2 Corning glass (1737F) substrates by RF magnetron sputtering from a 99.9% purity Al_2O_3 target (3 inch diameter). The gun is 3º tilted and located 10 cm off-axis of the substrate. The target to substrate distance was fixed at 15 cm and a substrate rotation of 10 rpm was used to achieve a better homogeneity during the deposition. The base pressure achieved before deposition was always between 2.7×10^{-4} Pa (2×10^{-6} Torr) and 4.0×10^{-4} Pa (3×10^{-6} Torr). The process working gas was 99.99% argon. In this work, we studied the effect of the RF power and the deposition pressure (exclusively argon gas) on the characteristics and properties of Al_2O_3 thin films deposited on the glass substrates. In the present study, the RF power values studied were 150, 300, and 450 W, while the studied deposition pressure values were 0.13 Pa (1.0 mTorr), 0.33 Pa (2.5 mTorr), and 0.67 Pa (5.0 mTorr).

A Dektak 3030 mechanical surface profiler, which is equipped with a 25 μm diameter probe, has been used to determine the thickness of the samples. In the deposited film, some steps were created by means of a simple lift-off technique. Thus, the depth of the steps could be precisely measured with the profiler, which has a vertical resolution of 1 nm. The obtained results were corroborated by confocal microscopy thanks to a Sensofar PLμ 2300 optical imaging profiler device. A first set of deposited films was measured to calculate the deposition rate under the two studied parameters, by assuming a constant deposition rate, and the results are plotted in **Figure 1**. The resulting values were used to calculate the deposition time required to obtain 50-nm thick thin films,

which is a common value used to passivate silicon wafers. This thickness of 50 nm was also corroborated in all the samples by means of the Sensofar PLμ 2300 optical imaging profiler device.

The percentage transmittance (*%T*) and percentage reflectance (*%R*) of the deposited 50-nm Al_2O_3 thin films were measured by using a Perkin Elmer Lambda 950 UV/Vis/NIR spectrophotometer in the 250 to 2500 nm wavelength interval. The percent transmittance was also integrated in the interval of 400 to 1100 nm in all the cases. The measurements were carried out with the Al_2O_3 thin films facing the incident light.

With the aim of finding some degree of crystallinity in the deposited Al_2O_3 material, the films were also measured by X-ray diffraction (XRD). Finally, the chemical bonding of the Al_2O_3 material was analyzed through X-ray photoelectron spectroscopy (XPS) by using a PHI 5500 Multitechnique system (from Physical Electronics), with a monochromatic X-ray source from Al Kα line with an energy of 1486.8 eV. The measured binding energies were charge-corrected by referencing the C 1*s* peak to 284.80 eV, which is usually assigned to the adventitious hydrocarbon [21a].

2.2. Al_2O_3 passivation effect on p-type c-Si wafers

In order to create a symmetrical structure, the Al_2O_3 thin films were deposited onto both sides of *p*-type *c*-Si wafers (high-quality float zone silicon wafers, 10 cm in diameter, 280 μm in thickness, and resistivity of 2.25 Ωcm). The deposition conditions were the same as previously described for the glass substrates. Before deposition, a careful cleaning process of the silicon wafer surface is critical to obtain high passivation values. The importance of this step lies on that the possible impurities remaining on the wafer surface would act as recombination centers. In this work the samples were initially cleaned using a two-steps standard wafer cleaning process (RCA sequence) [22]. The first step removes the organic surface contamination by means of a basic etching (RCA 1) with H_2O:H_2O_2:NH_3 (6:1:1) for 20 minutes at 70 ºC [23]. The second step removes the possible metal contamination of the surfaces with an acid etching (RCA 2) employing H_2O:H_2O_2:HCl (6:1:1) for 10 minutes at 70 ºC [24a]. Between RCA 1 and RCA 2 it is necessary a 60-s etching time in 1% hydrofluoric acid (HF) in order to remove the SiO_2 grown in the surface during the RCA 1. Finally, after the RCA 2 it is necessary another 60 s of immersion in 1% HF to remove the SiO_2 grown in the second RCA step. The depositions of Al_2O_3 were done immediately after finishing this last acid cleaning.

The performance of the sputtering-deposited Al_2O_3 as a passivation layer for *p*-Si wafers was evaluated from the effective lifetime of photogenerated carriers, which was measured by the quasi-steady-state photoconductance (QSSPC) technique with a Sinton WCT-120 instrument. The effective lifetime (τ_{eff}) of the minority carriers measured by the instrument can be related to recombination processes in the bulk and at the surfaces through the following equation [24b,25]:

$$\frac{1}{\tau_{\text{eff}}} = \frac{1}{\tau_{\text{bulk}}} + \frac{2S_{\text{eff}}}{W} \quad , \qquad (1)$$

where τ_{bulk} is the lifetime in the bulk, W is the wafer thickness (0.028 cm for the present case), and S_{eff} is the effective surface recombination velocity, that can be assumed equal on both sides of the symmetrical structure. For the high quality wafers used in this study (very long τ_{bulk}), the τ_{eff} is mainly limited by surface recombination, and the S_{eff} value can be obtained from:

$$S_{\text{eff}} \leq \frac{W}{2\tau_{\text{eff}}} \quad . \qquad (2)$$

Both measured τ_{eff} and calculated S_{eff} values were used to assess the passivation of the silicon wafers.

3. Results and discussion

The following text is divided into three subsections: the first one for the main characteristics of the Al_2O_3 layers deposited by sputtering on glass substrates and the second subsection for the surface passivation of the *p*-Si wafers with Al_2O_3; a third subsection is included for additional comments and future works.

3.1. Characteristics of the sputtering-deposited Al_2O_3 thin films

As shown in **Figure 1** (which was previously mentioned), it is observed that the deposition rate increases with the applied power, which is due to the higher energy introduced to the particles. On the other hand, the deposition rate decreases as the deposition pressure increases, due to the reduction of the mean free path when higher pressures are applied, which increases the number of particles in the plasma and therefore the probability of collisions. It is observed also that while the effect of the RF power was very significant in the deposition rate, the effect of deposition pressure was slight. Therefore, in the studied cases, the deposition rate is governed mainly by the deposition power.

At first sight, all the deposited Al_2O_3 thin films were completely transparent, with an appearance very similar to the glass substrate. It was observed through optical measurements that all the 50-nm Al_2O_3 thin films show very similar *%T* and *%R* values, independently of the RF power or deposition pressure. Some results of these measurements are presented in **Figure 2** and **Figure 3**, where, for the first case, the RF power was constant at 300 W and the deposition pressure was varied, and, for the second case, the deposition pressure was maintained constant at 0.667 Pa (5.0 mTorr) while the RF power was varied. In order to quantify the slight change in the *%T*, which seems to be mainly due to the increase in *%R*, as observed in the spectra, the measured values for *%T* were integrated in the interval of 400 to 1100 nm, by taking into account the absorption spectra of *c*-Si, and the results are presented in **Table 1**. The calculated values are around 91.5%, compared with the 94.1% corresponding to the uncovered glass substrate. These results confirm that the deposited Al_2O_3

material is very transparent, allowing the pass of the incident light to the substrate. As an additional comment, it is observed a slight increase in the calculated integrated *%T* when both the RF power and deposition pressure are increased, but the difference is not greater than ~0.8%.

All the deposited thin films were studied by means of XRD in order to determine any possible degree of crystallinity. **Figure 4** shows the diffractograms for the Al_2O_3 thin films deposited at 0.667 Pa (5.0 mTorr) and different RF powers, as examples. As it can be seen, it was not possible to detect any defined peak in the diffractograms, which implies that no crystallinity degree is found in the deposited 50-nm Al_2O_3. This amorphous nature was found in all the deposited films, regardless of the RF power or deposition pressure. On the other hand, in an attempt to determine whether this amorphous state could be attributed to the initial nucleation, which is dominant in very thin films, another Al_2O_3 film but with a thickness of 200 nm was deposited—in this case at 300 W, 0.667 Pa (5.0 mTorr), and again at room temperature—, but the recorded diffractogram was identical to those presented in **Figure 4**, which means that, for the studied conditions, the amorphous state is independent of the film thickness.

Concerning the chemical characteristics, an XPS analysis was carried out on all the samples with the aim of corroborating that the deposited material corresponds to the desired Al_2O_3, as well as to define the O/Al ratio for each sample. At first results, **Table 2** shows the location of the Al 2*p* and O 2*s* peaks maxima for all the deposited Al_2O_3 thin films before and after erosion with an argon ion sputtering during the XPS system operation. The locations of these peaks in the binding energy scale, whose mean values are 74.09 and 74.15 eV for the Al 2*p* before and after the erosion with argon ions, respectively, and 531.20 and 530.99 eV for the O 2*s*, also before and after the erosion treatment, fall in the position range compiled by Moulder *et al.* for the Al 2*p* [21b] and O 1*s* [21c] photoelectron lines. For a better comparison, and as examples for all the measured samples, the XPS spectra obtained before the erosion treatment on the surface of the Al_2O_3 thin films deposited at different pressure at 300 W are plotted in **Figure 5**, while those obtained for the films deposited at different RF power with the deposition pressure fixed at 0.67 Pa (5.0 mTorr) are shown in **Figure 6**. For both cases, all the characteristics XPS signals for aluminum and oxygen are clearly observed. Furthermore, it is important to note, for the first case, the appearance of argon signals as the deposition pressure decreases. **Figure 5(c)** clearly shows the Ar 2*p* peak (not deconvolutioned), which, among the three pressure values studied, takes importance when the Al_2O_3 thin films are deposited at 0.13 Pa (1.0 mTorr). Depositing the Al_2O_3 thin films at higher pressure values avoided the argon incorporation, as it can be seen in **Figure 6(c)**, in which the Ar 2*p* signals are absent at 0.67 Pa (5.0 mTorr), regardless of the RF power applied.

Regarding the deviation from the stoichiometry, **Figure 7** shows the O/Al ratio as a function of RF power at different deposition pressure values. This ratio was calculated from the XPS data recorded before and after the erosion treatment. It is observed in the figure that the O/Al ratio decreases with the increase of RF power, but increases with the deposition pressure. Thus, for the

studied parameters, the highest excess of oxygen (highest O/Al ratio) was achieved with a RF power of 150 W and a deposition pressure of 0.67 Pa (5.0 mTorr).

3.2. Results of silicon passivation with the sputtering-deposited Al_2O_3

Before addressing the passivation results of the *c*-Si wafers obtained with the sputtering-deposited Al_2O_3 thin films, two important points must be considered to help in the discussion of such results. First, it is well-known that the high-energy ions inherent to the sputtering process interact and modify in different ways the substrate surface [26–28]. One of the effects is the generation of lattice defects in the substrate surface, which can be considered a serious damage if the substrate is a semiconductor. However, besides of the increase of Q_f, one of the purposes of the passivation layers is precisely to diminish the interface traps, which seems to be the main problem limiting the level of surface passivation with layers deposited by sputtering. In this regard, the group of Cuevas [15,18] and Chen *et al.* [29] pointed out the importance of finding the proper sputtering parameters that can result in a reduction of the D_{it}. In certain way, this can be considered as a competition against the increase of D_{it} due to the ever-produced surface damage, inherent to the sputtering technique. On this point, we assume in advance that the increase in RF-power and the decrease of deposition pressure, which increases the energy of the particles and the probability to reach the substrate, respectively, lead to an increase in the silicon surface damage. Similar considerations were done by Cuevas and collaborators [15,18].

Second, it is also well-known that the passivation results obtained with the as-deposited Al_2O_3 thin films, regardless of the deposition technique employed, are very poor [2,3]. Therefore, an activation process by applying energy to the material is essential to fully optimize the surface passivation result. For the case of Al_2O_3 deposited by sputtering, it is suggested that such an activation, which is usually achieved by an annealing process, leads to an increase or restructuration of the SiO_x interfacial layer of the formed $Si/SiO_x/Al_2O_3$ structure, which improves both field-effect and chemical passivation by increasing Q_f [15,16,30] and reducing D_{it} [16,30], respectively. Furthermore, the annealing in ambient gasses containing hydrogen results beneficial to passivation due to an extra-reduction of D_{it} by hydrogenation of the silicon dangling bonds or the SiO_x interfacial layer [17,20].

Regarding the obtained passivation results, **Figure 8** and **Figure 9** show the measured τ_{eff} for the *p*-Si wafer uncovered and covered by the 50-nm Al_2O_3 thin films deposited, for the first case, at 300 W and different pressure values, and for the second case, at 0.67 Pa (5.0 mTorr) and different RF power values, both before and after an annealing process at 350 ºC for 20 min with forming gas. On the other hand, **Table 3** and **Table 4** depict the measured τ_{eff} and calculated S_{eff} values under one-sun illumination for both cases, respectively; the measured implied open circuit voltage (V_{oc}) is also presented. It can be observed a poor passivation result for all the as-prepared p-Si/Al_2O_3, regardless of the argon pressure or the RF power used for depositing the Al_2O_3 thin films, as expected. In the case in

which the RF power was varied with the argon pressure fixed at 0.67 Pa (5.0 mTorr), a very slight improvement (although in the bad passivation results range, with τ_{eff} values very close to that showed by the uncovered *p*-Si wafer) is achieved when the Al_2O_3 is deposited at high RF power values. Maybe the energy provided with the increase of this parameter slightly favored the formation or restructuration of the SiO_x interlayer. This change is not appreciable when the argon pressure is varied, maybe indicating that the results are mainly governed by the deposition power.

On the other hand, after the annealing process all the *p*-Si/Al_2O_3 reached the maximum passivation improvement, according to their full potential of optimization. It is observed that an increase of the τ_{eff} value—a decrease of S_{eff}—was obtained with the increase of the argon pressure and with a decrease of the RF power used for the deposition of the 50-nm Al_2O_3 thin films. The improved results achieved with the use of such conditions (high pressure and low power) can be related with a decrease in the surface damage, as expected. In the particular case of the argon pressure, higher values also avoid the incorporation of argon into the deposited Al_2O_3 material, although additional studies are necessary to determine the real effect of this contaminant. Thus, among the conditions studied in this work, the best τ_{eff} value at one-sun illumination, 0.34 ms, which corresponds to a S_{eff} of 41.2 cm/s, was obtained with the annealing of the *p*-Si covered with the Al_2O_3 deposited at 150 W and 0.67 Pa (5.0 mTorr). On the other hand, although the effect of the argon pressure is evident, the major changes in the passivation results are obtained with the change of the RF power applied during the deposition, thus confirming that the passivation results are governed by the deposition power. In this case, the decrease in the level of passivation with the increase of the RF power surely are associated to an increase of silicon surface damage produced at those conditions, as assumed previously, and also considered by the group of Cuevas [15,18] on the Al_2O_3 deposition by RF sputtering. Furthermore, this decrease in the passivation quality at higher RF power also coincides with the decrease of the O/Al ratio of the Al_2O_3 material, as it was observed in **Figure 7**. A similar correlation can be done with the decrease of the argon pressure, but the incorporation of argon in such conditions complicates a definitive conclusion. However, Li, Cuevas, and collaborators [16] sustained that the surface passivation results are not strongly dependent on the O/Al ratio of the deposited Al_2O_3 material, but on the formation or restructuration of the SiO_x interfacial layer. On the other hand, this correlation between O/Al and the passivation results is not completely discarded in the review wrote by Dingemans & Kessels [3], and a high O/Al ratio is probably related with the formation of the negative charge, especially if this O/Al ratio is high in the *p*-Si/(SiO_x)/Al_2O_3 interface.

Summarizing the above observation, the best surface passivation obtained at lower RF power and higher argon pressure can be related to a lower damage of the silicon surface, although the effect of the higher O/Al ratio must not be discarded. With the aim of fully corroborate such a correlation, we carried out a simple experiment with an Al_2O_3 thin film grown with deposition conditions that were continuously varied by starting from sputtering conditions that hypothetically lead to minimal surface damage. Such initial deposition conditions were 50 W and 6.67 Pa (50 mTorr), and the RF

power was later gradually increased while the deposition pressure was gradually decreased during the deposition, according to the details tabulated in **Table 5**, which were followed with the objective of increase the deposition rate and hence the thickness of the film. Here, we assumed that the initial deposited Al_2O_3 material serve mainly as a protective layer for the subsequent more aggressive conditions. By means of this method, we measured a τ_{eff} value of 0.73 ms, corresponding to a S_{eff} equal to 19.2 cm/s, at one-sun illumination after the annealing process at 350 ºC for 20 min with forming gas, thus corroborating all previous assumptions. The measured τ_{eff} as a function of the excess carrier density (Δn) for this sample, compared to the *p*-Si covered with the Al_2O_3 deposited at 150 W and 5.0 mTorr (the best for the series previously discussed), are plotted in **Figure 10**, whereas **Table 6** depicts the main data subtracted from the QSSPC measurement for both annealed samples. It is noteworthy that the value of 0.73 ms obtained with this preliminary experiment is to date the best τ_{eff} value reported for *p*-type *c*-Si passivated with Al_2O_3 deposited by sputtering. For a better comparison with the passivation results reported in literature, we show in **Table 7** the best τ_{eff} and S_{eff} recorded at an Δn equal to 1×10^{15} cm^{-3}, for which we obtained a τ_{eff} of 0.85 ms, corresponding to a S_{eff} of 16.5 cm/s.

3.3. Additional comments and future developments

All the surface passivation results presented in the previous section correspond to the usual values obtained under the studied conditions. However, we noted, qualitatively, that considerable variations in the manufacture process of the wafers, such as the cleaning process, exposure time to the air, humidity, and all these variations that obviously must be avoided, lead to a reduction of the surface passivation quality. For example, **Figure 11** shows some extreme values of surface passivation that can be obtained according to the previous consideration. In this specific case, in which the values must not be confused as statistical ones, we show the S_{eff} as a function of the studied RF power. An interesting observation arises from these results: the surface passivation is higher and easily reproduced when a low RF power is applied for depositing the Al_2O_3 thin films. This is other reason for applying a low RF power to deposit the passivation layers. However, the disadvantage of employing a lower RF power is the reduced deposition rate (see **Figure 1**); therefore, the experimenter must choose the deposition conditions according to the desired results.

By discarding the possible effect of the O/Al ratio (that is, the bulk characteristics of the Al_2O_3 layer) on the surface passivation results, and that the surface damage inherent to the sputtering technique is the main factor that reduces the passivation quality, some interesting passivation schemes can be designed. For example, in this context we assume that a very thin intermediate intrinsic layer of hydrogenated amorphous silicon (*a*-Si:H), deposited by plasma enhanced chemical vapor deposition (PE CVD) before the Al_2O_3 passivation thin film, can serve, on the one hand, as a physical protection layer to the bombardment with the high-energy ions produced during the subsequent sputtering process; and, on the other hand, can serve as a source of hydrogen atoms for surface chemical

passivation, in a similar way to the Al_2O_3 deposited by ALD. Advances in this passivation development, specifically with the *p*-Si/(~6-nm)*a*-Si:H/(50-nm)Al_2O_3 and *n*-Si/(~6-nm)*a*-Si:H/(50-nm)Al_2O_3 structures, in which the Al_2O_3 was deposited at 300 W and 0.67 Pa (5.0 mTorr), were recently presented in the 31st European Photovoltaic Solar Energy Conference and Exhibition (EU PVSEC 2015) [31]. By employing this intrinsic *a*-Si:H interlayer, we achieved, in such preliminary experiments, excellent τ_{eff} values of 1.25 ms (corresponding to a S_{eff} of 11.2 cm/s) and 1.42 ms (corresponding to a S_{eff} of 9.9 cm/s) for the *p*-Si and *n*-Si wafers, respectively. A systematical study of the use of this intrinsic *a*-Si:H interlayer, as well as experiments to define its main effect on the surface passivation results (either protective layer or hydrogen source), are currently in process.

Summarizing, all the results presented along this paper demonstrate that good surface passivation results can be obtained with solely Al_2O_3 thin films deposited by the industrially suitable sputtering technique, which depend on the deposition conditions. Additionally, there is a good potential to further improve such passivation results.

4. Conclusions

The Al_2O_3 thin films deposited at room temperature by RF magnetron sputtering are highly transparent and amorphous, independently of the RF power and argon deposition pressure, and even regardless of the film thickness.

The deposition of Al_2O_3 thin films at low argon pressure values can result in an incorporation of argon into the deposited films. This is evident for Al_2O_3 deposited at 0.13 Pa (1.0 mTorr), whereas the incorporation of argon at 0.67 Pa (5.0 mTorr) was not detected.

The O/Al ratio of the Al_2O_3 material increased with the deposition pressure and with the decrease of the RF power applied. Among the studied parameters, the highest O/Al ratio was obtained at 0.67 Pa (5.0 mTorr) and 150 W.

Bad surface passivation results were obtained with the as-deposited Al_2O_3 thin films, but they considerably improved after an annealing process, which is usually attributed to the formation or restructuration of a SiO_x interlayer, leading to an increase of Q_f and a decrease of D_{it}. The different surface passivation results obtained after the annealing process indicates that each sample shows a different potential of passivation, which depends on the overall deposition conditions.

The best surface passivation results are obtained by applying a low RF power and high argon pressure for depositing the Al_2O_3 thin films, which is attributed to a reduction of the surface damage inherent to the sputtering technique. Also, a probable effect of the higher O/Al ratio is not discarded.

Among the studied parameters, the best τ_{eff} value, 0.34 ms, to which corresponds an S_{eff} of 41 cm/s, is obtained after an annealing with forming gas at 350 ºC for 20 min (parameters not studied in this work) applied to the *p*-Si covered with 50-nm Al_2O_3 deposited at 150 W and 0.67 Pa (5.0 mTorr).

A simple experiment by employing a passivation film of Al_2O_3 deposited at initial very high argon pressure, 6.67 Pa (50 mTorr), and low RF power, 50 W, assumed as conditions that lead a minimal surface damage, provided a τ_{eff} value of 0.73 ms (a S_{eff} of 19 cm/s), thus corroborating that the silicon surface damage can be diminished with the proper sputtering conditions: high power and low pressure.

Therefore, the magnetron sputtering technique, which is nowadays completely integrated into the industry, is suitable for depositing Al_2O_3 passivation layers with good enough silicon surface passivation properties.

Acknowledgments

The *Centres Científics i Tecnològics de la Universitat de Barcelona* (CCiTUB) is acknowledged for the XRD and XPS measurements. The authors acknowledge the financial support by the *Ministerio de Economía y Competitividad* through the projects ENE2013-48629-C4-1-R and ENE2013-48629-C4-2-R, and J.A. García-Valenzuela acknowledges the financial support by the *Consejo Nacional de Ciencia y Tecnología* (CONACyT) with the registration numbers 208159 and 251082.

References

[1] B. Hoex, J. Schmidt, P. Pohl, M.C.M. van de Sanden, W.M.M. Kessels, Silicon surface passivation by atomic layer deposited Al_2O_3, J. Appl. Phys. 104 (4) (2008) 044903.

[2] G. Dingemans, W.M.M. Kessels, Recent progress in the development and understanding of silicon surface passivation by aluminum oxide for photovoltaics, EU PVSEC Proceedings, 2010, pp. 1083–1090, presented at: 25th European Photovoltaic Solar Energy Conference and Exhibition / 5th World Conference on Photovoltaic Energy Conversion (25th EU PVSEC / WCPEC-5), Valencia, Valencian Community, Spain, September 6–10, 2010.

[3] G. Dingemans, W.M.M. Kessels, Status and prospects of Al_2O_3-based surface passivation schemes for silicon solar cells, J. Vac. Sci. Technol. A 30 (4) (2012) 040802.

[4] M.Z. Rahman, S.I. Khan, Advances in surface passivation of c-Si solar cells, Mater. Renew. Sustain. Energy 1 (1) (2012) 1:1.

[5] S. Xiao, S. Xu, Status and progress of high-efficiency silicon solar cells, in: X. Wang, Z.M. Wang (Eds.), High-Efficiency Solar Cells — Physics, Materials, and Devices, Springer Series in Material Sciences, Volume 190, Springer Science+Business Media, 2014, pp. 1–58.

[6] G. Hahn, S. Joos, State-of-the-art industrial crystalline silicon solar cells, in: G.P. Willeke, E.R. Weber (Eds.), Semiconductors and Semimetals (Volume 90) — Advances in Photovoltaics: Part 3, Elsevier Inc., 2014, pp. 1–72.

[7] N. Balaji, S.Q. Hussain, C. Park, J. Raja, J. Yi, R. Jeyakumar, Surface passivation schemes for high-efficiency c-Si solar cells - A review, Trans. Electr. Electron. Mater. 16 (5) (2015) 227–233.

[8] J. Schmidt, F. Werner, B. Veith, D. Zielke, R. Bock, V. Tiba, P. Poodt, F. Roozeboom, [T.-T.]A. Li, A. Cuevas, R. Brendel, Industrially relevant Al_2O_3 deposition techniques for the surface passivation of Si solar cells, EU PVSEC Proceedings, 2010, pp. 1130–1133, presented at: 25th European Photovoltaic Solar Energy Conference and Exhibition / 5th World Conference on Photovoltaic Energy Conversion (25th EU PVSEC / WCPEC-5), Valencia, Valencian Community, Spain, September 6–10, 2010.

[9] J. Schmidt, F. Werner, B. Veith, D. Zielke, R. Bock, R. Brendel, V. Tiba, P. Poodt, F. Roozeboom, [T.-T.]A. Li, A. Cuevas, Surface passivation of silicon solar cells using industrially relevant Al_2O_3 deposition techniques, Photovoltaics International, Technical Papers, Edition 10 (2011) 52–57.

[10] J. Schmidt, F. Werner, B. Veith, D. Zielke, S. Steingrube, P.P. Altermatt, S. Gatz, T. Dullweber, R. Brendel, Advances in the surface passivation of silicon solar cells, Energy Procedia 15 (2012) 30–39.

[11] P. Saint-Cast, M. Hofmann, S. Kühnhold, D. Kania, L. Weiss, Y.-H. Heo, E. Billot, P. Olwal, D. Trogus, J. Rentsch, R. Preu, A review of PECVD aluminum oxide for surface passivation, EU PVSEC Proceedings, 2012, pp. 1797–1801, presented at: 27th European Photovoltaic Solar Energy Conference and Exhibition (27th EU PVSEC), Frankfurt, Hesse, Germany, September 24–28, 2012.

[12] G. Agostinelli, A. Delabie, P. Vitanov, Z. Alexieva, H.F.W. Dekkers, S. De Wolf, G. Beaucarne, Very low surface recombination velocities on p-type silicon wafers passivated with a dielectric with fixed negative charge, Sol. Energy Mater. Sol. Cells 90 (18–19) (2006) 3438–3443.

[13] B. Hoex, S.B.S. Heil, E. Langereis, M.C.M. van de Sanden, W.M.M. Kessels, Ultralow surface recombination of *c*-Si substrates passivated by plasma-assisted atomic layer deposited Al_2O_3, Appl. Phys. Lett. 89 (4) (2006) 042112.

[14] F. Werner, W. Stals, R. Görtzen, B. Veith, R. Brendel, J. Schmidt, High-rate atomic layer deposition of Al_2O_3 for the surface passivation of Si solar cells, Energy Procedia 8 (2011) 301–306.

[15] T.-T.[A.] Li, A. Cuevas, Effective surface passivation of crystalline silicon by rf sputtered aluminum oxide, phys. status solidi RRL 3 (5) (2009) 160–162.

[16] T.-T.A. Li, S. Ruffell, M. Tucci, Y. Mansoulié, C. Samundsett, S. De Iullis, L. Serenelli, A. Cuevas, Influence of oxygen on the sputtering of aluminum oxide for the surface passivation of crystalline silicon, Sol. Energy Mater. Sol. Cells 95 (1) (2011) 69–72.

[17] T.-T.A. Li, A. Cuevas, Role of hydrogen in the surface passivation of crystalline silicon by sputtered aluminum oxide, Prog. Photovolt: Res. Appl. 19 (3) (2011) 320–325.

[18] X. Zhang, A. Cuevas, A. Thomson, Process control of reactive sputter deposition of AlO_x and improved surface passivation of crystalline silicon, IEEE J. Photovolt. 3(1) (2013) 183–188.

[19] X. Zhang, A. Cuevas, Plasma hydrogenated, reactively sputtered aluminum oxide for silicon surface passivation, phys. status solidi RRL 7 (9) (2013) 619–622.

[20] X. Zhang, A. Thomson, A. Cuevas, Silicon surface passivation by sputtered aluminum oxide: influence of annealing temperature and ambient gas, ECS Solid State Lett. 3 (11) (2014) N37–N39.

[21] J.F. Moulder, W.F. Stickle, P.E. Sobol, K.D. Bomben, in: J. Chastain, R.C. King Jr. (Eds.), Handbook of X-Ray Photoelectron Spectroscopy — A Reference Book of Standard Spectra for Identification and Interpretation of XPS Data, Physical Electronics, Inc. Eden Praire, Minnesota, USA, 1995 , pp. (a) 14,22,33, (b) 55, (c) 45.

[22] W. Kern, D.A. Puotinen, Cleaning solutions based on hydrogen peroxide for use in silicon semiconductor technology, RCA Review 31 (1970) 187–206.

[23] K. Yamamoto, A. Nakamura, U. Hase, Control of cleaning performance of an ammonia and hydrogen peroxide mixture (APM) on the basis of a kinetic reaction model, IEEE Trans. Semicond. Manuf. 12 (3) (1999) 288–294.

[24] A.G. Aberle, Crystalline Silicon Solar Cells: Advanced Surface Passivation and Analysis, Centre for Photovoltaic Engineering, University of New South Wales, Sidney, Australia, 1999.

[25] J. Schmidt, A.G. Aberle, Accurate method for the determination of bulk minority-carrier lifetimes of mono- and multicrystalline silicon wafers, J. Appl. Phys. 81 (9) (1997) 6186–6199.

[26] D.M. Mattox, Particle bombardment effects on thin-film deposition: A review, J. Vac. Sci. Technol. A 7 (3) (1989) 1105–1114.

[27] M. Ohring, Discharges, plasmas, and ion-surface interactions, in: Materials Science of Thin Films, 2nd Ed., Academic Press, 2001, pp. 145–202.

[28] D.M. Mattox, Physical sputtering and sputter deposition (Sputtering), in: Handbook of Physical Vapor Deposition (PVD) Processing, 2nd Ed., Elsevier Inc., 2010, pp. 237–286.

[29] S. Chen, L. Tao, L. Zeng, R. Hong, RF magnetron sputtering aluminum oxide film for surface passivation on crystalline silicon wafers, Int. J. Photoenergy 2013 (2013) 792357.

[30] M. Bhaisare, A. Misra, A. Kottantharayil, Aluminum oxide deposited by pulsed-DC reactive sputtering for crystalline silicon surface passivation, IEEE J. Photovolt. 3 (3) (2013) 930–935.

[31] J.A. García-Valenzuela, A. Caballero, J.M. Asensi, J. Bertomeu, J. Andreu, L.G. Gerling-Sarabia, A.B. Morales[-Vilches], P. Ortega, C. Voz, Intermediate amorphous silicon layer for crystalline silicon passivation with alumina, EU PVSEC Proceedings, 2015, pp. 719–723, presented at: 31st European Photovoltaic Solar Energy Conference and Exhibition (EU PVSEC 2015), Hamburg, Germany, September 14–18, 2015.

[32] M. Bhaisare, D. Sutar, A. Misra, A. Kottantharayil, Effect of power density on the passivation quality of pulsed - DC reactive sputtered aluminium oxide on p - type crystalline silicon, 2013

IEEE 39th Photovoltaic Specialists Conference (PVSC), 2013, pp. 1207–1211, presented at: 2013 IEEE 39th Photovoltaic Specialists Conference (PVSC), Tampa, Florida, USA, June 16–21, 2013.

[33] R. Kotipalli, R. Delamare, F. Henry, J. Proost, D. Flandre, Thermal stability analysis of DC-sputtered Al_2O_3 films for surface passivation of c-Si solar cells, EU PVSEC Proceedings, 2013, pp. 1278–1281, presented at: 28th European Photovoltaic Solar Energy Conference and Exhibition (28th EU PVSEC), Paris, France, September 30 – October 4, 2013.

Table captions

Table 1. Integrated *%T* calculated in the interval from 400 to 1100 nm for the Al_2O_3 thin films deposited on glass substrate at different RF power and deposition pressure values; the *%T* value calculated for the glass substrate is 94.1%.

Table 2. Binding energy positions of the Al 2*p* and O 1*s* peaks maxima for the Al_2O_3 deposited on glass substrate at different RF power and deposition pressure; values at the left of the arrow correspond to the Al_2O_3 surface as is, while values at the right correspond to those recorded after 1-min erosion with argon ion sputtering.

Table 3. Effective lifetime, surface recombination velocity, and implied open circuit voltage values measured or calculated under one-sun illumination for the as-prepared and annealed *p*-Si samples uncovered and covered with the Al_2O_3 thin films deposited at different argon pressure values at a RF power of 300 W.

Table 4. Effective lifetime, surface recombination velocity, and implied open circuit voltage values measured or calculated under one-sun illumination for the as-prepared and annealed *p*-Si samples uncovered and covered with the Al_2O_3 thin films deposited at different RF power values at a deposition pressure of 0.67 Pa (5.0 mTorr).

Table 5. Details for the conditions followed to continuously depositing Al_2O_3 starting from minimal surface damage conditions.

Table 6. Effective lifetime, surface recombination velocity, and implied open circuit voltage values measured or calculated under one-sun illumination for the annealed *p*-Si samples covered with the Al_2O_3 thin films deposited at 150 W and 0.67 Pa (5.0 mTorr), for the first case, and under minimal surface damage conditions, for the second case.

Table 7. Best effective lifetime and surface recombination velocity values obtained on annealed *p*-type *c*-Si wafers passivated with Al_2O_3 deposited by sputtering (under conditions without intentionally added hydrogen), according to the reported in literature for an excess carrier density of 1×10^{15} cm^{-3}.

Figure captions

Figure 1. Variation of the calculated deposition rate of the Al_2O_3 thin films as a function of the RF power for different deposition pressure values, by using mechanically and optically measured data.

Figure 2. Percent transmittance and percent reflectance spectra of the glass substrate uncovered and covered with the Al_2O_3 thin films deposited at different pressure values at a RF power of 300 W.

Figure 3. Percent transmittance and percent reflectance spectra of the glass substrate uncovered and covered with the Al_2O_3 thin films deposited at different RF power values at a deposition pressure of 0.67 Pa (5.0 mTorr).

Figure 4. X-ray diffractograms of the Al_2O_3 thin films deposited on glass substrate at different RF power values at a deposition pressure of 0.67 Pa (5.0 mTorr).

Figure 5. X-ray photoelectron spectra of the non-eroded Al_2O_3 thin films deposited on glass substrate at different pressure values at a RF power of 300 W for (a) the survey interval, (b) the high-resolution O 1*s* region, (c) the Ar 2*p* region, and (d) the high-resolution Al 2*p* region.

Figure 6. X-ray photoelectron spectra of the non-eroded Al_2O_3 thin films deposited on glass substrate at different RF power values at a deposition pressure of 0.67 Pa (5.0 mTorr) for (a) the survey interval, (b) the high-resolution O 1*s* region, (c) the Ar 2*p* region, and (d) the high-resolution Al 2*p* region.

Figure 7. Variation of the O/Al ratio of the Al_2O_3 material as a function of the RF power for different deposition pressure values, calculated from the X-ray photoelectron spectroscopy data measured before and after the 1-min erosion treatment with an argon ion sputtering.

Figure 8. Variation of the effective lifetime of the as-prepared and annealed *p*-Si samples uncovered and covered with the Al_2O_3 thin films deposited at different argon pressure values at a RF power of 300 W, expressed as a function of the excess carrier density.

Figure 9. Variation of the effective lifetime of the as-prepared and annealed *p*-Si samples uncovered and covered with the Al_2O_3 thin films deposited at different RF power values at a deposition pressure of 0.67 Pa (5.0 mTorr), expressed as a function of the excess carrier density.

Figure 10. Variation of the effective lifetime of the annealed *p*-Si samples uncovered and covered with the Al_2O_3 thin films deposited at 150 W and 0.67 Pa (5.0 mTorr), for one case, and under minimal surface damage conditions, for the best case.

Figure 11. Variation of the effective surface recombination velocity due to certain changes in the manufacture process; the results are plotted as a function of RF power and correspond to those calculated after the annealing process.

Table 1

Table 1. Integrated *%T* calculated in the interval from 400 to 1100 nm for the Al_2O_3 thin films deposited on glass substrate at different RF power and deposition pressure values; the *%T* value calculated for the glass substrate is 94.1%.

RF power (W)	Deposition pressure (Pa)	Recorded voltage (V)	Integrated *%T* (%)
150	0.13 (1.0 mTorr)	60–40	90.8
150	0.33 (2.5 mTorr)	61–43	91.3
150	0.67 (5.0 mTorr)	62–45	91.6
300	0.13 (1.0 mTorr)	172–150	91.2
300	0.33 (2.5 mTorr)	152–138	91.4
300	0.67 (5.0 mTorr)	160–150	91.8
450	0.13 (1.0 mTorr)	271–263	91.5
450	0.33 (2.5 mTorr)	220–211	91.7
450	0.67 (5.0 mTorr)	231–225	91.8

Table 2

Table 2. Binding energy positions of the Al 2*p* and O 1*s* peaks maxima for the Al_2O_3 deposited on glass substrate at different RF power and deposition pressure; values at the left of the arrow correspond to the Al_2O_3 surface as is, while values at the right correspond to those recorded after 1-min erosion with argon ion sputtering.

RF power (W)	Deposition pressure (Pa)	Al 2*p* peak position (eV)	O 1*s* peak position (eV)
150	0.13 (1.0 mTorr)	74.12 → 74.17	531.18 → 530.97
150	0.67 (5.0 mTorr)	74.08 → 74.17	531.37 → 531.14
300	0.13 (1.0 mTorr)	74.14 → 74.14	531.34 → 531.12
300	0.33 (2.5 mTorr)	74.00 → 74.21	531.09 → 530.92
300	0.67 (5.0 mTorr)	74.06 → 74.10	531.25 → 530.85
450	0.13 (1.0 mTorr)	74.15 → 74.14	531.07 → 530.97
450	0.67 (5.0 mTorr)	74.09 → 74.10	531.13 → 530.93

Table 3

Table 3. Effective lifetime, surface recombination velocity, and implied open circuit voltage values measured or calculated under one-sun illumination for the as-prepared and annealed *p*-Si samples uncovered and covered with the Al_2O_3 thin films deposited at different argon pressure values at a RF power of 300 W.

Sample	Effective lifetime, τ_{eff} (μs)		Effective surface recombination velocity, S_{eff} (cm/s)		Implied open circuit voltage, V_{oc} (mV)	
	As-prepared	Annealed	As-prepared	Annealed	As-prepared	Annealed
p-Si	0.682	0.816	20,530	17,150	513.8	518.5
p-Si/Al_2O_3 at 0.13 Pa, 140–119 V	1.01	173	13,860	80.92	518.8	654.1
p-Si/Al_2O_3 at 0.33 Pa, 134–116 V	1.06	185	13,080	75.68	519.3	656.1
p-Si/Al_2O_3 at 0.67 Pa, 152–133 V	1.05	275	13,330	50.95	519.6	674.5

Table 4

Table 4. Effective lifetime, surface recombination velocity, and implied open circuit voltage values measured or calculated under one-sun illumination for the as-prepared and annealed *p*-Si samples uncovered and covered with the Al_2O_3 thin films deposited at different RF power values at a deposition pressure of 0.67 Pa (5.0 mTorr).

Sample	Effective lifetime, τ_{eff} (μs)		Effective surface recombination velocity, S_{eff} (cm/s)		Implied open circuit voltage, V_{oc} (mV)	
	As-prepared	Annealed	As-prepared	Annealed	As-prepared	Annealed
p-Si	0.682	0.816	20,530	17,150	513.8	518.5
p-Si/Al_2O_3 at 150 W, 48–25 V	0.779	340	17,980	41.22	515.1	682.2
p-Si/Al_2O_3 at 300 W, 134–109 V	0.936	275	14,950	50.95	519.6	674.5
p-Si/Al_2O_3 at 450 W, 221–192 V	1.54	135	9,110	103.5	536.0	651.5

Table 5

Table 5. Details for the conditions followed to continuously depositing Al_2O_3 starting from minimal surface damage conditions.

RF power (W)	Deposition pressure (Pa)	Time (min)	Accumulated time (min)
50	6.67 (50.0 mTorr)	5	5
50	5.33 (40.0 mTorr)	25	30
50 – 60	5.33 – 4.00 (40.0 – 30.0 mTorr)	2	32
60	4.00 (30.0 mTorr))	5	37
60 – 70	4.00 – 2.67 (30.0 – 20.0 mTorr)	2	39
70	2.67 (20.0 mTorr)	5	44
70 – 80	2.67 – 2.00 (20.0 – 15.0 mTorr)	2	46
80	2.00 (15.0 mTorr)	3	49
80 – 90	2.00 – 0.93 (15.0 – 7.0 mTorr)	2	51
90	0.93 (7.0 mTorr)	2	53
90 – 100	0.93 – 0.67 (7.0 – 5.0 mTorr)	2	55
100	0.67 (5.0 mTorr)	2	57
100 – 150	0.67 (5.0 mTorr)	8	65
150	0.67 (5.0 mTorr)	55	120

Table 6. Effective lifetime, surface recombination velocity, and implied open circuit voltage values measured or calculated under one-sun illumination for the annealed *p*-Si samples covered with the Al_2O_3 thin films deposited at 150 W and 0.67 Pa (5.0 mTorr), for the first case, and under minimal surface damage conditions, for the second case.

Sample	Effective lifetime, τ_{eff} (μs)	Effective surface recombination velocity, S_{eff} (cm/s)	Implied open circuit voltage, V_{oc} (mV)
p-Si/Al_2O_3 at 130 W and 5.0 mTorr	340	41.22	682.2
p-Si/Al_2O_3 at minimal surface damage	728	19.23	708.2

Table 7

Table 7. Best effective lifetime and surface recombination velocity values obtained on annealed *p*-type *c*-Si wafers passivated with Al_2O_3 deposited by sputtering (under conditions without intentionally added hydrogen), according to the reported in literature for an excess carrier density of 1×10^{15} cm^{-3}.

Year, authors	Annealing conditions	Effective lifetime, τ_{eff} (μs)	Effective surface recombination velocity, S_{eff} (cm/s)
2009, Li & Cuevas [15]	N_2, 400 ºC, 60 min	227 [a]	74 [b]
2009, Li & Cuevas [15]	Forming gas, 400 ºC, 60 min	292 [a]	55 [b]
2010, Schmidt, Li, Cuevas, *et al.* [8]	400±50 ºC, 15 min	425 [a]	35 [b]
2011, Schmidt, Li, Cuevas, *et al.* [9]	400±50 ºC, 15 min	425 [a]	35 [b]
2011, Li, Cuevas, *et al.* [16]	N_2, 400 ºC, 180 min	212 [c]	73 [a]
2012, Schmidt *et al.* [10]	400±50 ºC, 15 min	425 [a]	35 [b]
2013, Chen *et al.* [29]	N_2, 500 ºC, 30 min	135 [b]	-
2013, Bhaisare *et al.* [30]	N_2 or N_2+O_2, 520 ºC	324 [a]	44 [a]
2013, Bhaisare *et al.* [32]	N_2+O_2, 520 ºC	390 [a]	38 [a]
2013, Kotipalli *et al.* [33]	Forming gas, 430 ºC, 30 min	49 [a]	200 [c]
2015, García-Valenzuela *et al.* [31]	Forming gas, 350 ºC, 20 min	46 [a,d]	307 [a,d]
2016, García-Valenzuela *et al.*, this work	Forming gas, 350 ºC, 20 min	851 [d]	16.5 [d]

[a] Value subtracted from the plots reported in the paper.

[b] Value numerically reported in the paper.

[c] Value calculated from data given in the paper.

[d] Value given as a preliminary result.

Figures 1

Click here to download Figures (if any): Fig. 1. Dep Rate vs Power and Pressure.docx

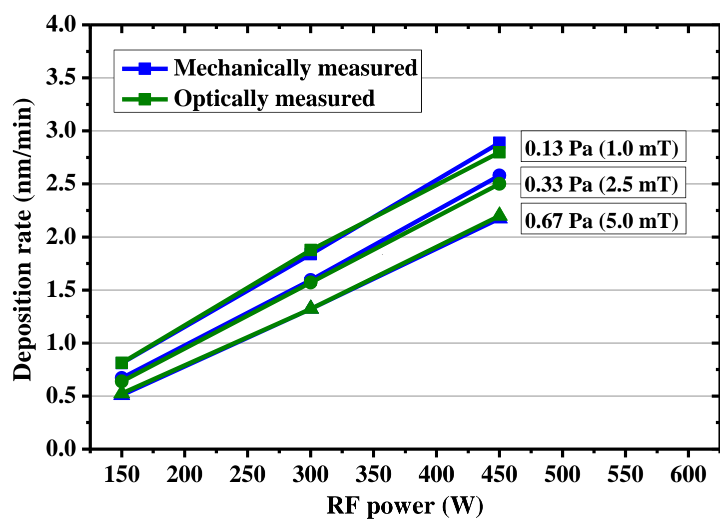

Figures 2

Click here to download Figures (if any): Fig. 2. RT at 5mTorr.docx

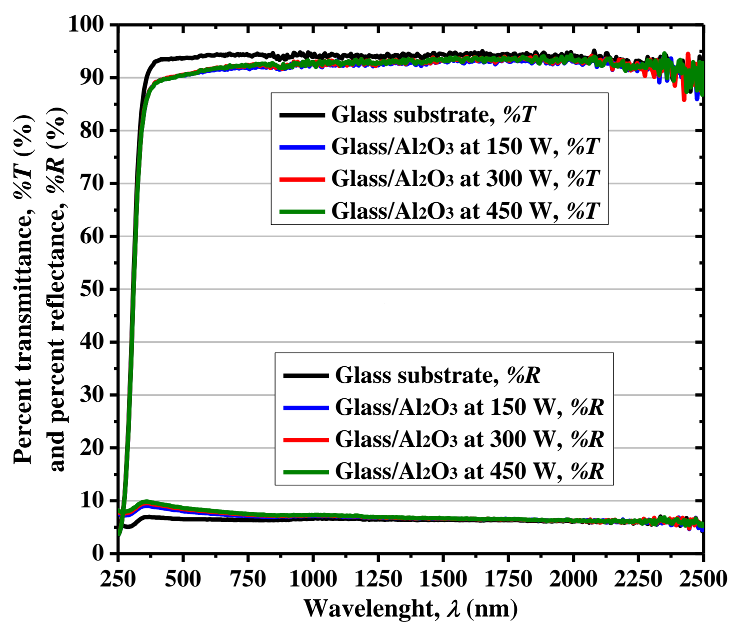

Figures 3

Click here to download Figures (if any): Fig. 3. RT at 300W.docx

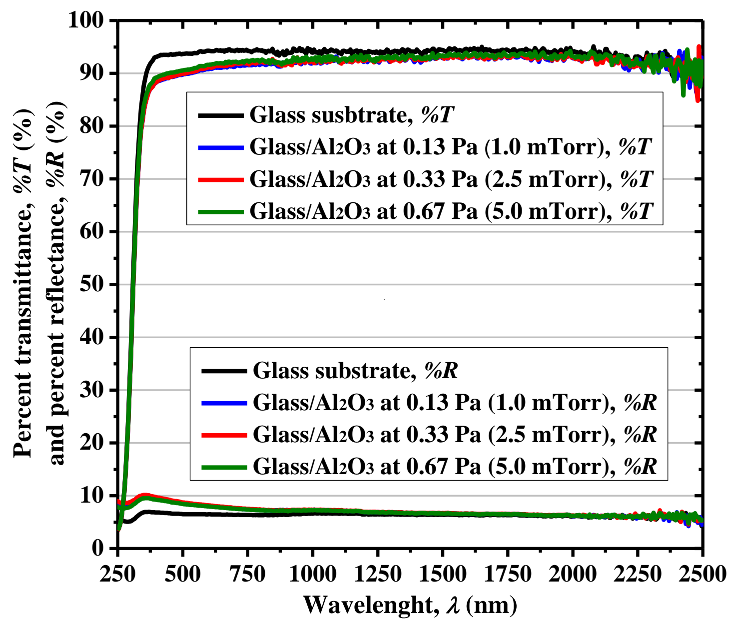

Figures 4

Click here to download Figures (if any): Fig. 4. XRD at 5mT.docx

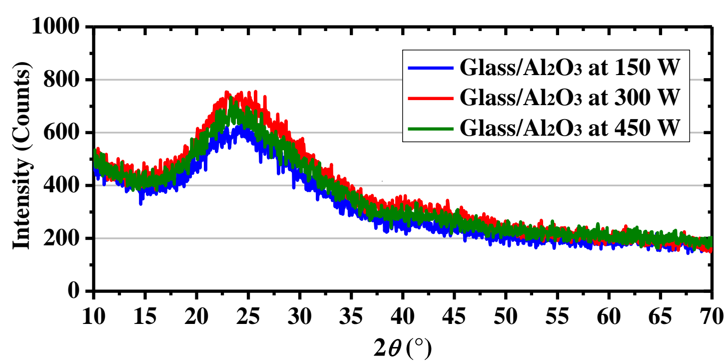

Figures 5

Click here to download Figures (if any): Fig. 5. XPS at 300W.docx

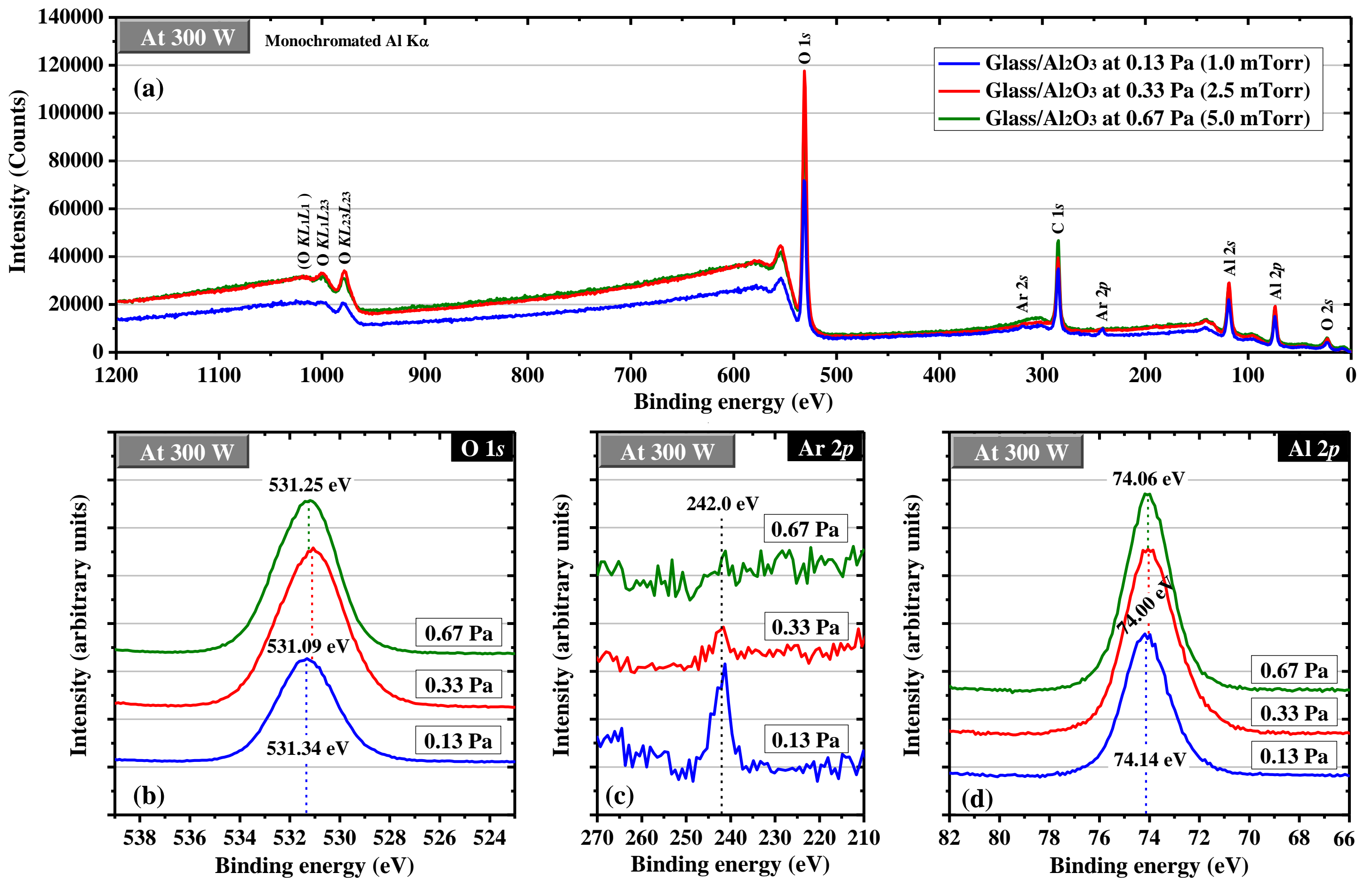

Figures 6

Click here to download Figures (if any): Fig. 6. XPS at 5mT.docx

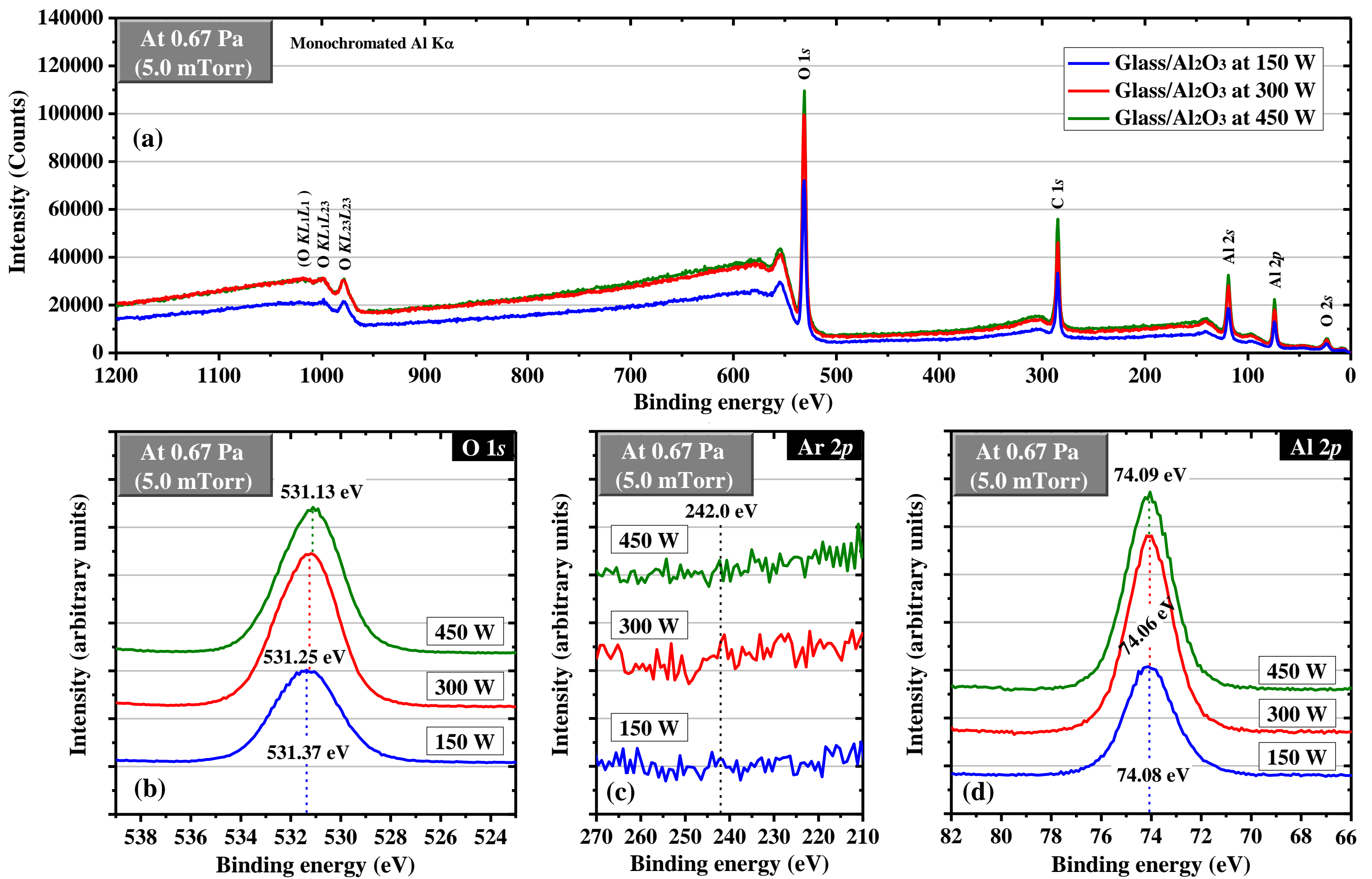

Figures 7

Click here to download Figures (if any): Fig. 7. O-Al Ratio vs Power and Pressure.docx

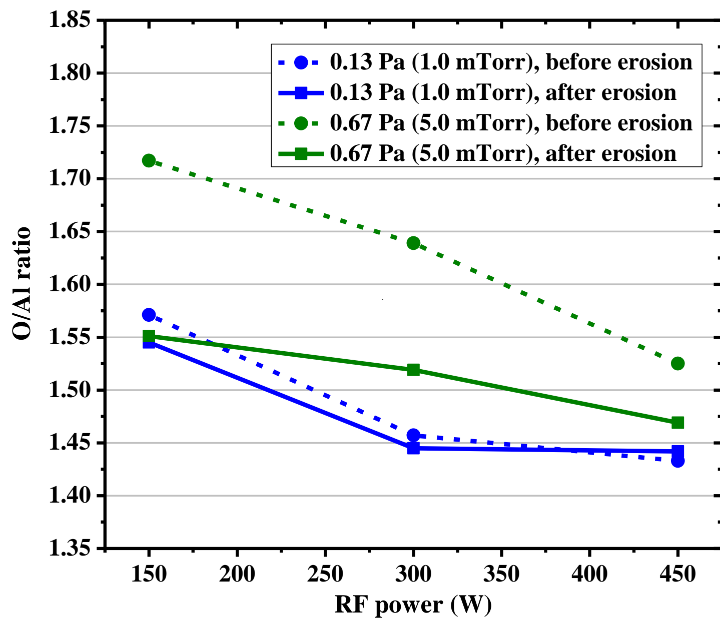

Figures 8

Click here to download Figures (if any): Fig. 8. Lifetime at 300W.docx

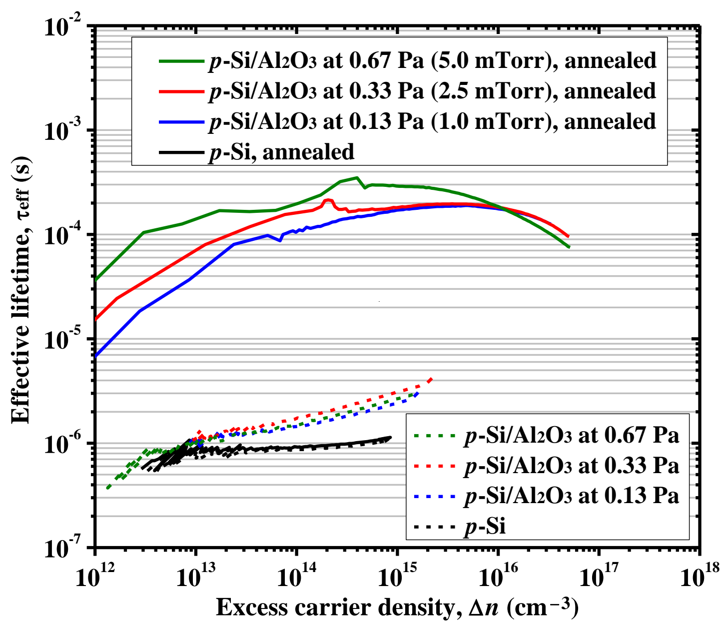

Figures 9

Click here to download Figures (if any): Fig. 9. Lifetime at 5mTorr.docx

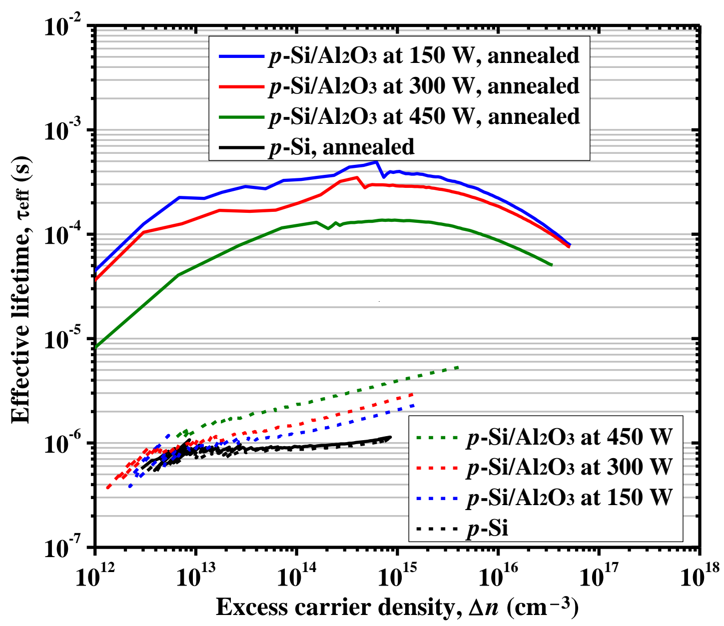

Figures 10

Click here to download Figures (if any): Fig. 10. Lifetime at Minimal Damage Conditions.docx

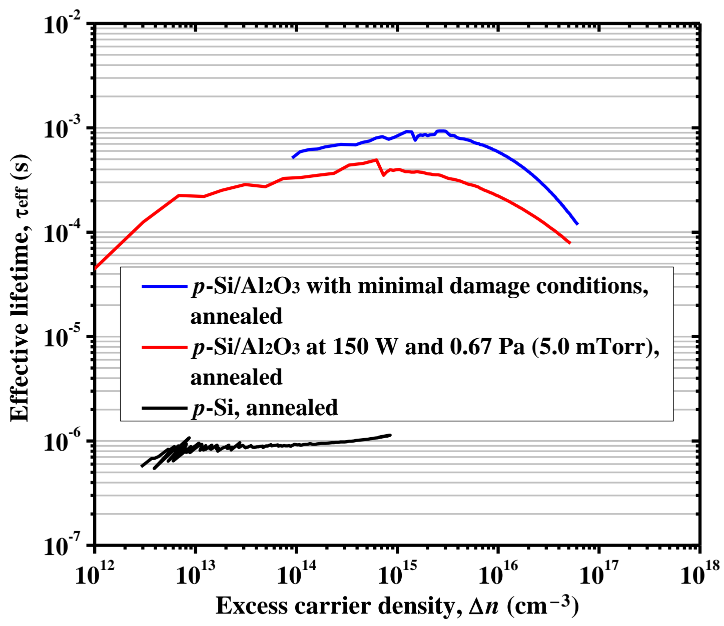

Figures 11

Click here to download Figures (if any): Fig. 11. Variation of Surface Recombination Velocities.docx